Twin-Tapered Molecules Containing Bi-dihydrazine Units: Self-Assembly through Intermolecular Quadruple Hydrogen Bonding and Liquid Crystalline Behavior

Songnan Qu, Fan Li, Haitao Wang, Binglian Bai, Chunyan Xu, Lianjiu Zhao, Beihong Long, and Min Li*

Key Laboratory for Automobile Materials (JLU), Ministry of Education, Institute of Materials Science and Engineering, Jilin University, Changchun 130012, P. R. China

Received October 30, 2006. Revised Manuscript Received July 5, 2007

We report on the synthesis and self-assembly of a new series of twin-tapered dihydrazide derivatives, oxalyl acid *N*′,*N*′-di(3,4,5-trialkoxybenzoyl)-hydrazide (FH-Tn). Results from ^{1}H NMR diluting experiments in chloroform and temperature-dependent ^{1}H NMR spectroscopy revealed that molecules exhibited a conformational change at concentrations lower than 255 μM, e.g., from intramolecularly H-bonded six-membered rings to five-membered rings in the monomer state upon concentrating. Measurements of ^{1}H NMR diluting experiment, FTIR spectroscopy, and mass spectroscopy revealed that the FH-Tn self-assembled into supramolecular chains either in chloroform at concentrations greater than 255 μM or in bulk through intermolecular quadruple H-bonding. On the basis of the results of DSC, polarized optical microscopy, and wide-angle X-ray diffraction (WAXD), we assigned enantiotropic hexagonal and unknown columnar phases to FH-Tn (n = 6, 7, 8, 10).

Introduction

Molecule self-assembly through noncovalent interactions into various superstructures opens new possibilities in the fields of both biology and materials science.[1] Among the noncovalent interactions, hydrogen bonds are one of the most important interactions in the self-assembly of molecules because of their strength, directionality, reversibility, and selectivity. Multiply (>3) hydrogen-bonded modules were demonstrated to be powerful assembling tools because of their increased bonding strength, specificity, and directionality, and have found extensive applications in the construction of superstructures.[2,1f] Since Meijer and co-workers first reported a series of 2-ureido-4(1*H*)-pyrimidone derivatives that can dimerize through intermolecular quadruple hydrogen bonds,[3] quadruply hydrogen-bonded systems have attracted much attention and have been used in the field of materials science to synthesize, for the first time, supramolecular polymers through the self-association of self-complementary monomers.[4] Generally, two types of modes, e.g., non-self-complementary binding and self-complementary binding, can be used to construct quadruple hydrogen-bonding motifs. The non-self-complementary binding arrays are ideal tools to selectively assemble specific heterodimeric systems,[5] but have the drawback that very precise control over stoichiometry is required to obtain high degrees of polymerization. In the quadruple hydrogen-bonding motifs, the ADAD−DADA and AADD−DDAA (A = hydrogen-bond acceptor, D = hydrogen-bond donor) arrays are self-complementary, which offers distinct advantages in the self-assembly of supramolecular polymers.[6,1f] However, the number of the self-complementary quadruple hydrogen-bonding units available for use is limited.[6,1f,2h] Therefore, there is a strong need to develop new types of self-complementary quadruple hydrogen-bonding units.

* Corresponding author. Fax: 86 431 5168444. E-mail: minli@mail.jlu.edu.cn.

(1) (a) Special issue on "Supramolecular Chemistry & Self-Assembly" *Science* **2002**, *295*, 2313−2556. (b) Kato, T. *Science* **2002**, *295*, 2414−2418. (c) Davis, J. T. *Angew. Chem.* **2004**, *116*, 684−716; *Angew. Chem., Int. Ed.* **2004**, *43*, 668−698. (d) Gottarelli, G.; Spada, G. P.; Garbesi, A. In *Comprehensive Supramolecular Chemistry*; Lehn, J.-M., Atwood, J. L., Davies, J. E. D., MacNicol, D. D., Vötle, F., Sauvage, J.-P., Hosseini, M. W., Eds.; Pergamon: Oxford, 1996; pp 483−506; Vol. 5. (e) Gottarelli, G.; Spada, G. P. *Chem. Rev.* **2004**, *4*, 39−49. (f) Brunsveld, L.; Folmer, B. J. B.; Meijer, E. W.; Sijbesma, R. P. *Chem. Rev.* **2001**, *101*, 4071−4097. (g) Muthukumar, M.; Ober, C. K.; Thomas, E. L. *Science* **1997**, *277*, 1225−1232. (h) Stupp, S. I.; LeBonheur, V.; Walker, K., Li, L. S.; Huggins, K. E.; Keser, M.; Amstutz, A. *Science* **1997**, *276*, 384−389.

(2) (a) Lüning, U.; Kühl, C. *Tetrahedron Lett.* **1998**, *39*, 5735. (b) Beijer, F. H.; Kooijman, H.; Spek, A. L.; Sijbesma, R. P.; Meijer, E. W. *Angew. Chem., Int. Ed.* **1998**, *37*, 75. (c) Sessler, J. L.; Wang, R. *Angew. Chem., Int. Ed.* **1998**, *37*, 1726. (d) Beijer, F. H.; Sijbesma, R. P.; Kooijman, H.; Spek, A. L.; Meijer, E. W. *J. Am. Chem. Soc.* **1998**, *120*, 6761. (e) Corbin, P. S.; Zimmerman, S. C. *J. Am. Chem. Soc.* **1998**, *120*, 9710. (f) Gong, B.; Yan, Y.; Zeng, H.; Skrzypczak-Jankunn, E.; Kim, Y. W.; Zhu, J.; Ickes, H. *J. Am. Chem. Soc.* **1999**, *121*, 5607. (g) Schmuck, C.; Wienand, W. *Angew. Chem., Int. Ed.* **2001**, *40*, 4363. (h) Sijbesma, R. P.; Meijer, E. W. *Chem. Commun.* **2003**, 5.

(3) (a) Beijer, F. H.; Kooijman, H.; Spek, A. L.; Sijbesma, R. P.; Meijer, E. W. *Angew. Chem.* **1998**, *110*, 79−82; *Angew. Chem., Int. Ed.* **1998**, *37*, 75−78. (b) Beijer, F. H.; Sijbesma, R. P.; Kooijman, H.; Spek, A. L.; Meijer, E. W. *J. Am. Chem. Soc.* **1998**, *120*, 6761−6769.

(4) Sijbesma, R. P.; Beijer, F. H.; Brunsveld, L.; Folmer, B. J. B.; Ky Hirschberg, J. H.; Lange, R. F. M.; Lowe, J. K. L.; Meijer, E. W. *Science* **1997**, *278*, 1601−1604.

(5) (a) Corbin, P. S.; Zimmerman, S. C.; Thiessen, P. A.; Hawryluk, N. A.; Murray, T. J. *J. Am. Chem. Soc.* **2001**, *123*, 10475. (b) Brammer, S.; Lüning, U.; Kühl, C. *Eur. J. Org. Chem.* **2002**, 4054. (c) Zeng, H.; Yang, X.; Flowers, R. A.; Gong, B. *J. Am. Chem. Soc.* **2002**, *124*, 2903. (d) Zhao, X.; Wang, X.-Z.; Jiang, X.-K.; Chen, Y.-Q.; Li, Z.-T.; Chen, G.-J. *J. Am. Chem. Soc.* **2003**, *125*, 15128.

(6) (a) Zimmermann, S. C.; Corbin, P. S. *Struct. Bonding (Berlin)* **2000**, 63−94. (b) Schmuck, C.; Wienand, W. *Angew. Chem., Int. Ed.* **2001**, *40*, 4363.

10.1021/cm062581i CCC: $37.00
Published on Web 09/08/2007

Columnar liquid crystals are well-known examples of supramolecular assemblies based on self-organization and have received considerable interest as functional materials for applications.[7−9] Hydrogen bonding has been used to either organize discotic molecules[10] or to arrange multiple precursors to form discs that can then self-assemble to columns.[11] Hydrogen bonding between amide groups has been utilized to build supramolecular architectures and columnar supramolecules consisting of peptide, urea, hydrazine, or dihydrazine groups.[12] Recently, Percec et al. reported on a novel architectural concept and a strategy to design LC superlattices based on twin-tapered molecules containing twin-dendritic benzamides and polymers containing twin-dendritic benzamide side groups.[13] Cheng et al. reported discotic LC phases from symmetric-tapered bisamides based on an amide core of 1,2-bis[3,4,5-tris(alkan-1-yloxy)benzamido]benzene and three alkyl tails on each side of the core.[14] Especially, a ferroelectric columnar phase of *N,N′*-bis(3,4,5-trialkoxylphenyl)ureas, which are chemically symmetric and contain amide groups in the central core and multiple alkyl tails linking at the ends of the rigid core, was reported by Kishikawa.[15]

Hydrazide units have been used to build supramolecular liquid crystals[12,16] and to control the folding structures of artificial peptides.[17] Li and co-workers reported a new class of highly stable hydrazide-based ADDA−DAAD heterodimers, which represented the first successful application of hydrazide derivatives in the self-assembly of hydrogen-mediated supramolecular systems with well-established structures.[5d] In our previous work, we have demonstrated that lateral H-bonding based on dihydrazine groups in calamitic mesogenic materials may enhance the parallel alignment and thus stabilize the smectic phase.[16b] Herein, we report the design, synthesis and the self-assembling behaviors of a novel twin-tapered compounds, which contain bi-dihydrazine phenyl as a rigid core with three alkoxyl tails at each end of the core (FH-Tn, $n = 3, 6, 7, 8, 10$). The novelty of the present work is: (1) a new type of self-complementary quadruple hydrogen-bonding module based on bi-dihydrazine groups was designed and has been demonstrated to be useful for the construction of supramolecules; (2) quadruple hydrogen-bonding was introduced into twin-tapered molecules and conformational transitions in monomers were detected through the ^{1}H NMR diluting experiment; (3) enantiotropic columnar phases were observed in FH-Tn ($n = 6, 7, 8, 10$) and room-temperature column hexagonal phases were obtained by air-drying the chloroform solutions of FH-T6 and FH-T7. Our present results suggested that intermolecular quadruple H-bonding among bi-dihydrazine units, which is the main driving force for FH-Tn molecules to form supramolecular chains either in solution or in bulk, could be used as self-complementary quadruple hydrogen-bonding units to assemble new supramolecules.

Scheme 1. Synthetic Route of FH-Tn

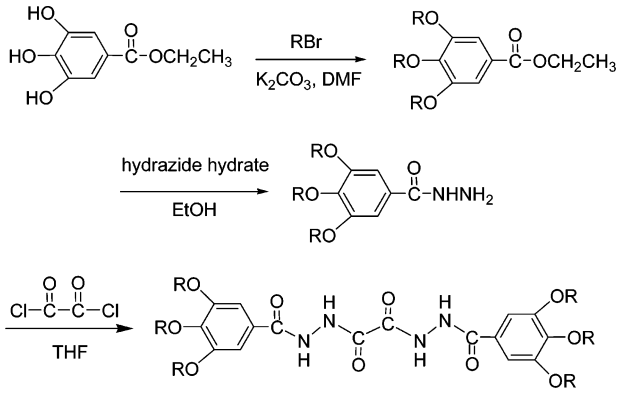

FH-T3: R= $-(CH_2)_2CH_3$ FH-T6: R= $-(CH_2)_5CH_3$ FH-T7: R= $-(CH_2)_6CH_3$
FH-T8: R= $-(CH_2)_7CH_3$ FH-T10: R= $-(CH_2)_{10}CH_3$

Experimental Section

Synthesis. All commercially available chemicals were of reagent grade and were used without further purification. 3,4,5-Trihydroxy benzoic acid ethyl ester, oxalyl chloride, and 1-bromide alkyl were purchased. 3,4,5-Trialkoxy-benzoyl hydrazine was prepared according to the literature procedures.[18] THF was dried by standard technique. The compounds were synthesized according to the route shown in Scheme 1. Oxalyl chloride (11 mmol) was regularly injected into the THF solution of 3,4,5-trialkoxy-benzoyl hydrazine

(7) Photovoltaic solar cells: (a) Nelson, J. *Science* **2001**, *293*, 1059−1060. (b) Schmidt-Mende, L.; Fechtenkötter, A.; Müllen, K.; Moons, E.; Friend, R. H.; MacKenzie, J. D. *Science* **2001**, *293*, 1119−1122. (c) Schmidt-Mende, L.; Watson, M.; Müllen, K.; Friend, R. H. *Mol. Cryst. Liq. Cryst.* **2003**, *396*, 73−90. (d) Hassheider, T.; Benning, S. A.; Lauhof, M. W.; Kitzerow, H. S.; Bock, H.; Watson, M. D.; Müllen, K. *Mol. Cryst. Liq. Cryst.* **2004**, *413*, 461−472. (e) Oukachmih, M.; Destruel, P.; Seguy, I.; Ablart, G.; Jolinat, P.; Archambeau, S.; Mabiala, M.; Fouet, S.; Bock, H. *Sol. Energy Mater. Sol. Cells* **2005**, *85*, 535−543.

(8) Light emitting diodes: (a) Freudenmann, R.; Behnisch, B.; Hanack, M. *J. Mater. Chem.* **2001**, *11*, 1618−1624. (b) Bayer, A.; Zimmermann, S.; Wendorff, J. H. *Mol. Cryst. Liq. Cryst.* **2003**, *396*, 1−22.

(9) Field effect transistors: (a) van de Craats, A. M.; Stutzmann, N.; Bunk, O.; Nielsen, M. M.; Watson, M.; Müllen, K.; Chanzy, H. D.; Sirringhaus, H.; Friend, R. H. *Adv. Mater.* **2003**, *15*, 495−499. (b) Katsuhara, M.; Aoyagi, I.; Nakajima, H.; Mori, T.; Kambayashi, T.; Ofuji, M.; Takanishi, Y.; Ishikawa, K.; Takezoe, H.; Hosono, H. *Synth. Met.* **2005**, *149*, 219−223.

(10) (a) Paulus, W.; Ringsdorf, H.; Diele, S.; Pelzl, G. *Liq. Cryst.* **1991**, *9*, 807−819. (b) Shu, W.; Valiyaveettil, S. *Chem. Commun.* **2002**, 1350−1351.

(11) (a) Kleppinger, R.; Lillya, P.; Yang, C. *J. Am. Chem. Soc.* **1997**, *119*, 4097−4102. (b) Suarez, M.; Lehn, J. M.; Zimmermann, S. C.; Skoulios, A.; Heinrich, B. *J. Am. Chem. Soc.* **1998**, *120*, 9526−32. (c) Yang, W.; Chai, X.; Chi, L.; Liu, X.; Cao, Y.; Lu, R.; Jiang, Y.; Tang, X.; Fuchs, H.; Li, T. *Chem.—Eur. J.* **1999**, *5*, 1144−1149. (d) Kraft, A.; Reichert, A.; Kleppinger, R. *Chem. Commun.* **2000**, 1015. (e) Kanie, K.; Yasuda, T.; Ujiie, S.; Kato, T. *Chem. Commun.* **2000**, 1891.

(12) Beginn, U. *Prog. Polym. Sci.* **2003**, *28*, 1049−1105.

(13) (a) Percec, V.; Ahn, C. H.; Bera, T. K.; Ungar, G.; Yeardley, D. J. P. *Chem.—Eur. J.* **1999**, *5*, 1070. (b) Percec, V.; Bera, T. K.; Glodde, M.; Fu, Q.; Balagurusamy, V. S. K.; Heiney, P. A. *Chem.—Eur. J.* **2003**, *9*, 921−935.

(14) (a) Xue, C.; Jin, S.; Weng, X.; Ge, J. J.; Shen, Z.; Shen, H.; Graham, M. J.; Jeong, K.-U.; Wang, H.; Zhang, D.; Guo, M.; Harris, F. W.; Cheng, S. Z. D.; Li, C. Y.; Zhu, L. *Chem. Mater.* **2004**, *16*, 1014. (b) Shen, H.; Jeong, K. U.; Xiong, H.; Graham, M. J.; Leng, S.; Zheng, J. X.; Huang, H.; Guo, M.; Harris, F. W.; Cheng, S. Z. D. *Soft Matter* **2006**, *2*, 232.

(15) (a) Kishikawa, K.; Nakahara, S.; Nishikawa, Y.; Kohmoto, S.; Yamamoto, M. *J. Am. Chem. Soc.* **2005**, *127*, 2565. (b) Okada, Y.; Matsumoto, S.; Takanishi, Y.; Ishikawa, K.; Nakahara, S.; Kishikawa, K.; Takezoe, H. *Phys. Rev. E* **2005**, *72*, 020701(R).

(16) (a) Kutsumizu, S. *Curr. Opin. Solid State* **2002**, *6*, 537. (b) D. Pang, H. Wang, M. Li, *Tetrahedron* **2005**, *61*, 6108−6114.

(17) (a) Nowick, J. S.; Smith, E. M.; Pairish, M. *Chem. Soc. Rev.* **1996**, *25*, 401. (b) Soth, M. J.; Nowick, J. S. *Curr. Opin. Chem. Biol.* **1997**, *1*, 120. (c) Nowick, J. S. *Acc. Chem. Res.* **1999**, *32*, 287.

(18) Zhang, Y. D.; Jespersen, K. G.; Kempe, M.; Kornfield, J. A.; Barlow, S.; Kippelen, B.; Marder, S. R. *Langmuir* **2003**, *19*, 6534.

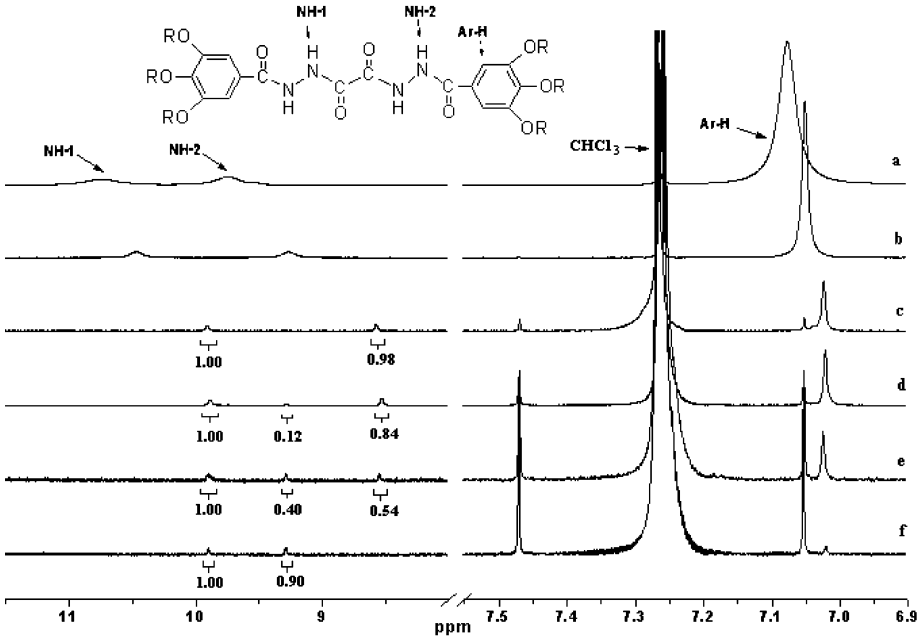

Figure 1. Partial proton NMR spectra (500 MHz, $CDCl_3$, 25 °C) of FH-T7 at different concentrations: (a) 101, (b) 8.32, (c) 0.255, (d) 0.120, (e) 0.045, and (f) 0.023 mM (the numbers indicate the relative integral area of the protons).

(23 mmol) with vigorous stirring at room temperature for 8 h, yielding the products of FH-Tn. All the compounds were purified by a recrystallization from alcohol for further NMR and FT-IR spectroscopy and elemental analysis.

Oxalyl Acid *N*′,*N*′-Di(3,4,5-propyloxybenzoyl)-hydrazide. ^{1}H NMR (300 MHz, $CDCl_3$, 25 °C, TMS): δ 10.29 (s, 2H), 9.14 (s, 2H), 7.06 (s, 4H), 3.96 (s, 4H), 3.88 (s, 8H), 1.76 (s,12H), 1.03−1.00 (m, 18H). FT-IR: ν 3255, 3152, 3074, 2965, 2938, 2878, 1719, 1686, 1631, 1584, 1547, 1468, 1428, 1386, 1338, 1300, 1219, 1261, 1219, 1113, 1060, 1000, 960, 856, 837, 790, 751, 602 cm^{-1}. Anal. Calcd (%) for $C_{34}H_{50}N_4O_{10}$: C, 60.52; H, 7.47; N, 8.30. Found: C, 60.59; H, 7.54; N, 8.31.

Oxalyl Acid *N*′,*N*′-Di(3,4,5-hexyloxybenzoyl)-hydrazide. ^{1}H NMR (300 MHz, $CDCl_3$, 25 TMS): δ 10.53 (s, 2H), 9.42 (s, 2H), 7.06 (s, 4H), 3.97−3.84 (m, 12H), 1.71−1.66 (m, 12H), 1.45−1.28 (m, 36H), 0.91−0.85 (m, 18H). FT-IR: ν 3338, 3211, 3013, 2957, 2932, 2872, 2860, 1719, 1695, 1624, 1582, 1467, 1427, 1386, 1337, 1234, 1216, 1001, 1043, 926, 859, 750, 777, 726 cm^{-1}; Anal. Calcd (%) for $C_{52}H_{86}N_4O_{10}$: C, 67.36; H, 9.35; N, 6.04. Found: C, 67.58; H, 9.45; N, 5.79.

Oxalyl Acid *N*′,*N*′Ddi(3,4,5-heptyloxybenzoyl)-hydrazide. ^{1}H NMR (500 MHz, $CDCl_3$, 25 °C, TMS): δ 10.15 (s, 2H), 8.90 (s, 2H), 7.03 (s, 4H), 4.03−3.94 (m, 12H), 1.81−1.71 (m, 12H), 1.50−1.42 (m, 12H), 1.35−1.30 (m, 36H), 0.89 (t, 18H, J = 6.5 Hz). ^{13}C NMR (300 MHz, $CDCl_3$): δ 165.08, 155.21, 153.18, 142.05, 125.31, 105.89, 73.44, 69.17, 31.90, 31.87, 31.81, 30.36, 29.37, 29.24, 29.12, 26.05, 26.01, 25.95, 22.65, 22.62, 14.06. FT-IR: ν 3214, 3016, 2956, 2928, 2871, 2857, 1693, 1629, 1580, 1468, 1428, 1384, 1336, 1234 , 1212, 1114, 1004, 857, 750, 720 cm^{-1}. Anal. Calcd (%) for $C_{58}H_{98}N_4O_{10}$: C, 68.88; H, 9.77; N, 5.54. Found: C, 69.16; H, 10.05; N, 5.47.

Oxalyl Acid *N*′,*N*′-Di(3,4,5-octanoxybenzoyl)-hydrazide. ^{1}H NMR (300 MHz, $CDCl_3$, 25 °C, TMS): δ 10.35 (s, 2H), 9.15 (s, 2H), 7.04 (s, 4H), 4.00−3.88 (m, 12H), 1.76−1.67 (m, 12H), 1.42−1.28 (m, 60H), 0.89 (t, 18H, J = 6.5 Hz); FT-IR: ν = 3213, 2957, 2926, 2856, 1692, 1629, 1582, 1468, 1427, 1386, 1336, 1231, 1218, 1115, 1007, 957, 858, 782, 750, 722, 601 cm^{-1}. Anal. Calcd (%) for $C_{64}H_{110}N_4O_{10}$: C ,70.16; H, 10.12; N, 5.11. Found: C, 70.35; H, 10.09; N, 4.85.

Oxalyl Acid *N*′,*N*′-Di(3,4,5-decyloxybenzoyl)-hydrazide. ^{1}H NMR (300 MHz, $CDCl_3$, 25 °C, TMS): δ 10.31 (s, 2H), 9.08 (s, 2H), 7.04 (s, 4H), 4.02−3.91 (m, 12H), 1.77−1.68 (m, 12H), 1.43−1.26 (m, 84H), 0.86 (t, 18H, J = 6.6 Hz). FT-IR: ν 3233, 3013, 2955, 2924, 2854, 1693, 1630, 1583, 1487, 1468, 1428, 1385, 1338, 1234, 1211, 1116, 1001, 987, 932, 857, 782, 751, 721, 601 cm^{-1}. Anal. Calcd (%) for $C_{76}H_{134}N_4O_{10}$: C, 72.22; H, 10.69; N, 4.43. Found: C, 72.23; H, 10.92; N, 4.50.

Characterization. ^{1}H NMR spectra were recorded with a Bruker Avance 500 MHz or VARIAN 300 MHz spectrometer, using chloroform-*d* as solvent and tetramethylsilane (TMS) as an internal standard (δ = 0.00). ^{13}C NMR spectra were recorded with a VARIAN 300 MHz spectrometer, using chloroform-*d* as solvent and $CDCl_3$ as an internal standard (δ = 77.00). Mass spectra were obtained by MALDI-TOF mass spectrometry. FT-IR spectra were recorded with a Perkin−Elmer spectrometer (Spectrum One B). The samples were pressed tablet with KBr. Phase transitional properties were investigated by Mettler Star DSC 821^e. Optical textures were observed under a Leica DMLP microscope equipped with a Leitz 350 heating stage. X-ray diffraction was carried out with a Bruker Avance D8 X-ray diffractometer.

Results and Discussion

Self-Assembly Behaviors in Solution. To understand the self-assembly behaviors of FH-Tn, we carried out ^{1}H NMR diluting experiments for FH-T7 in $CDCl_3$ at 25 °C (Figure 1). The assignment of the NH signals of FH-Tn in ^{1}H NMR spectra was based on 2D-NOESY experiments (see the Supporting Information). At 0.023 mM, peaks of NH-1 (near to bi-carbonyl group, 9.90 ppm) and NH-2 (near to alkoxy phenyl, 9.28 ppm) in FH-T7 were sharp, and Ar−H was observed at 7.02 ppm. Upon concentrating from 23 to 255 μM, no significant change ($\Delta\delta$ < 0.03) was observed for NH-1 signals (at about 9.90), whereas an obvious split was observed for NH-2. The NH-2 signal at 9.28 ppm decreased (about 43% at 45 μM to zero at 255 μM), and that at 8.53 ppm increased (57% at 45 μM to 100% at 255 μM) with a

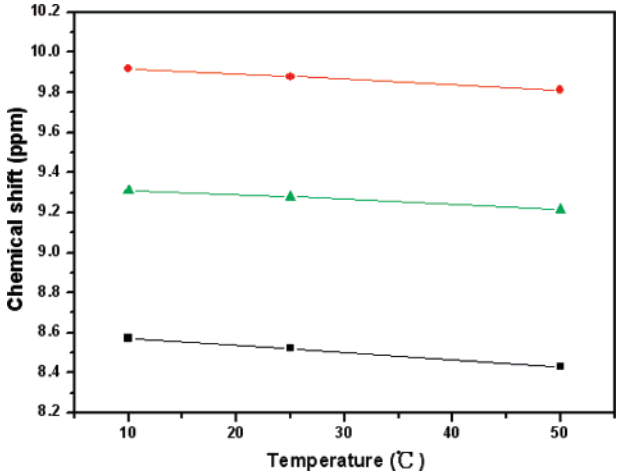

Figure 2. Chemical shifts of NH-1 (●), NH-2 (▲), and (■) FH-T7 at 120 μM in $CDCl_3$ vs temperature.

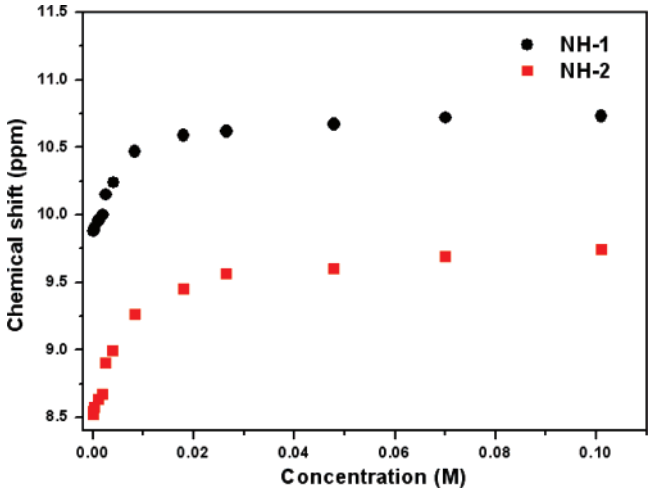

Figure 3. Concentration dependence of the chemical shifts of NH-1 and NH-2 in the ^1H NMR spectra of FH-T7 in $CDCl_3$.

Scheme 2. Two Possible Intramolecular Hydrogen-Bonding Patterns of Bi-dihydrazide Unit in FH-Tn in CDCl3 at Concentrations Lower than 255 μM (the dashed line illustrates the hydrogen bonding)

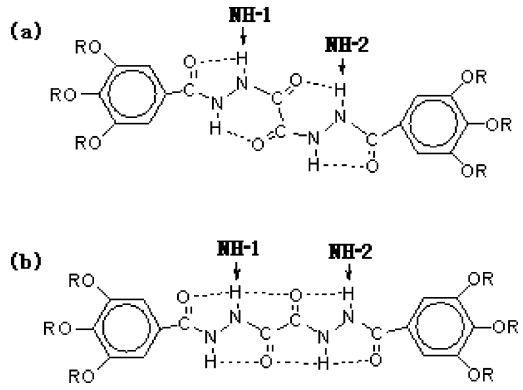

slight downfield shift ($\Delta\delta$ = 0.04). The NH-2 signal at 9.28 ppm disappeared and all that appeared at 8.57 ppm at 255 μM. Considering that the chemical shifts in nuclear magnetic resonance spectroscopy represent time averages of atoms at the same chemical environment, the split of NH-2 signals might indicate that a conformational change took place in FH-T7 during concentrating from 23 to 255 μM.

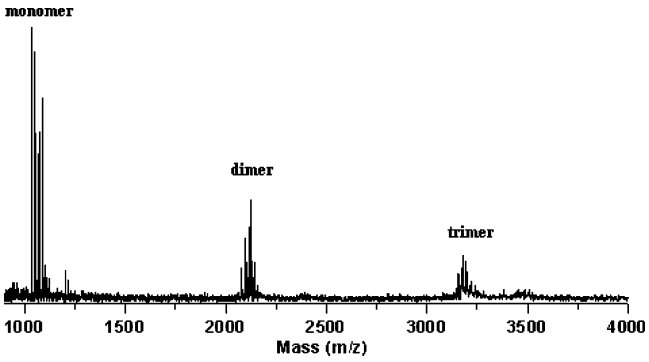

Figure 4. Partial MALDI-TOF mass spectrum of FH-T7 using chloroform as solvent.

Scheme 3. Schematic Representation of FH-Tn Self-Assembling to Supramolecules (the dashed line illustrates the hydrogen bonding)

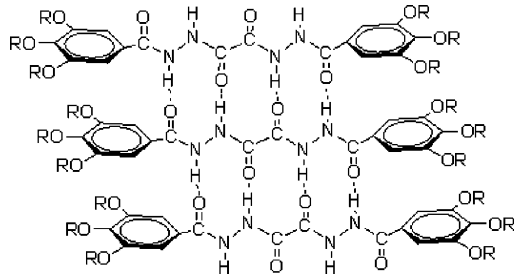

The chemical shifts of both NH-1 at 9.90 ppm and NH-2 at 9.28 ppm of FH-T7 showed concentration independence at concentrations lower than 120 μM, indicating their monomeric feature. The chemical shifts of NH-1 and NH-2 in FH-T7 versus temperature in $CDCl_3$ at 120 μM are shown in Figure 2. The NH-1 signal at 9.90 ppm and the NH-2 signals at 9.28 and 8.53 ppm, which are 2.63×10^{-3} ppm K^{-1}, 2.42×10^{-3} ppm K^{-1} and 3.54×10^{-3} ppm K^{-1} respectively, exhibited weak temperature dependence, suggesting that they were all involved in intramolecular H-bonding at 120 μM.[19] Thus, it can be concluded that the NH-2 signal at 8.53 ppm was assigned to monomer. At this stage, however, we don't have further experimental evidence to give the real conformational changes in monomers. It seemed that the split of NH-2 signals was associated with a change in the intramolecular H-bonding patterns of bi-dihydrazide unit in monomers. Two possible intramolecular H-bonding patterns of the bi-dihydrazide unit are illustrated in Scheme 2. In pattern a, protons of both NH-1 and NH-2 were involved in intramolecular hydrogen bonding with C═O groups, forming two five-membered rings and two six-membered rings, respectively. In pattern b, protons of both of NH-1 and NH-2 were all bonded to −C═O groups, forming five-membered rings. Considering that a six-

(19) (a) Hamuro, Y.; Geib, S. J.; Hamilto, A. D. *J. Am. Chem. Soc.* **1996**, *118*, 7529−7541. (b) Hamuro, Y.; Geib, S. J.; Hamilto, A. D. *J. Am. Chem. Soc.* **1997**, *119*, 10587−7541. The chemical shifts of both NH-1 and NH-2 exhibited much greater temperature dependence, e.g., 1.40×10^{-2} ppm K^{-1} for NH-1 and 1.76×10^{-2} ppm K^{-1} for NH-2 at 6.7 mM, at which intermolecular H-bonding has been demonstrated. If the NH-2 signal at 9.28 ppm belongs to a state that is very strongly bound to water in $CDCl_3$, this bonding will not be destroyed if there is enough water. Considering that the molar percentage of water in 120 μM FH-T7 in CDCl3 was excessive compared to NH-2 of FH-T7 (see the Supporting Information), the possibility of the NH-2 signal at 9.28 ppm belonging to a state bonding to water can be eliminated.

Table 1. Phase transition temperatures (*T*, °C) and enthalpies (Δ*H*, kJ mol^{-1}, in brackets)[a] of FH-Tn (*n* = 3, 6, 7, 8, 10)

	heating		cooling	
compd	phase	*T* (°C) (Δ*H* (kJ mol^{-1}))	phase	*T* (°C) (Δ*H* (kJ mol^{-1}))
FH-T3	Cr_1-Cr_2	143 (6.09)	Cr_2-Cr_1	133 (5.90)
	Cr_2-I	238 (19.82)	$I-Cr_2$	230 (20.06)
FH-T6	Col_x-Col_h	130.9 (8.56)	Col_h-Col_x	117.6 (7.33)
	Col_h-I	195.6 (6.90)	$I-Col_h$	192.1 (6.94)
FH-T7	$G-Col_x$	99.8		
	Col_x-Col_h	117.5 (3.92)	Col_h-Col_x	109.9 (3.78)
	Col_h-I	177.3 (6.56)	$I-Col_h$	176.8 (6.48)
FH-T8	$G-Col_x$	91.8		
	Col_x-Col_h	111.7 (4.35)	Col_h-Col_x	107.2 (4.09)
	Col_h-I	162.1 (4.79)	$I-Col_h$	157.8 (5.05)
FH-T10	$G-Col_x$	105.8	Col_x-G	102.3
	Col_x-Col_h	117.2 (4.18)	Col_h-Col_x	116.9 (4.11)
	Col_h-I	144.5 (5.88)	$I-Col_h$	142.7 (5.94)

[a] I, isotropic; Col_h, hexagonal columnar phase; G, glass; Col_x, unknown columnar phase, and Cr_1, Cr_2, crystalline.

membered ring is more favorable than a five-membered one for NH-2 forming intramolecular hydrogen bonding with the C═O group,[20] it was reasonable to propose that protons of NH-2 at 9.28 ppm belonged to six-membered-ring H-bonding, whereas those at 8.53 ppm were attributed to five-membered rings for concentrations between 23 and 255 μM. Further more, pattern b is more favorable than pattern a for intermolecular H-bonding. On the basis of the discussion above, we assumed that at concentration lower than 23 μM, the bi-dihydrazide unit in monomer adopted pattern a and exhibited a conformational change from pattern a to pattern b upon concentrating to 255 μM.

Further increasing concentrations of FH-T7 in $CDCl_3$ from 255 μM to 101 mM led to remarkable broadening and a continuous downfield shift of both NH-1 (Δδ = 0.83) and NH-2 (Δδ = 1.22), and a small downfield shift (Δδ = 0.05) of the Ar−H signal. The dependence of the chemical shifts of NH-1 and NH-2 in FH-T7 on concentrations is shown in Figure 3. The chemical shift of NH-1 and NH-2 increased almost linearly with increasing concentration and then slowed down and appeared to level off at 26 mM. The above results demonstrated that the two kinds of amide protons in FH-T7 cooperatively participated in forming supramolecules via intermolecular quadruple hydrogen bonds, which are the main driving force for supramolecular aggregation at higher concentrations. The association constant for FH-T7 was estimated using the simplest (isodesmic) model (i.e., $K_n = K$, for $n \geq 2$) from eq 1

$$KC_T = (P - P_\alpha)(P_\xi - P_\alpha)/(P_\xi - P)^2 \qquad (1)$$

Where P_α and P_ξ are the chemical shifts for monomers and molecules within a stack, P is the observed chemical shift, K is the association constant, and C_T is total molar concentration of the compounds.[21] In the present case, P_α was assigned to 8.53 and 9.90 ppm on the basis of NH-1 and NH-2, respectively. The data from the diluting experiment fit well with the calculated curves, giving association constants (K) of 447.5 and 217.2 M^{-1} on the basis of NH-1 and NH-2, respectively.

(20) Steiner, T. *Angew. Chem., Int. Ed.* **2002**, *41*, 48−76.
(21) Martin, R. B. *Chem. Rev.* **1996**, *96*, 3043−3064.

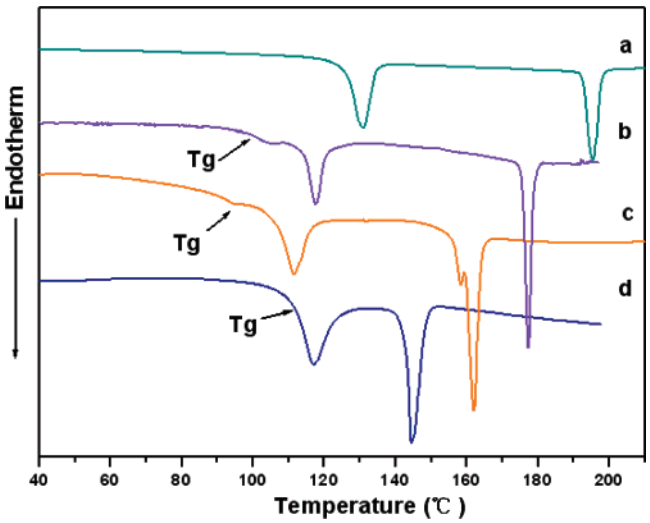

Figure 5. DSC curves of (a) FH-T6, (b) FH-T7, (c) FH-T8, and (d) FH-T10 on the second heating run (heating rate: 10 °C/min).

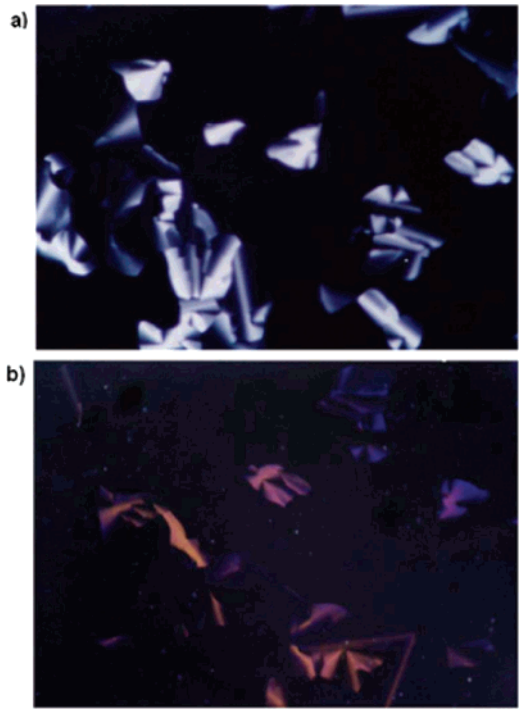

Figure 6. Optical textures observed for FH-T7 at (a) 150 °C (×200) and (b) 30°C (×200).

The MALDI-TOF mass spectrum of FH-T7 also provided support for the formation of the supramolecules in chloroform (Figure 4). Six peaks for the monomer M_1: *m/z* 1034.1 $[M_1 + Na]^+$, 1050.0 $[M_1 + Ka]^+$, 1056.2 $[M_1 + 2Na - H]^+$, 1066.1 $[M_1 + 2Na + Ka - 2CH_3]^+$, 1072.1 $[M_1 + Na + Ka - H]^+$ and 1088.1 $[M_1 + 2Ka - H]^+$. Seven peaks for dimmer M_2: *m/z* 2077.0 $[M_2 + 2Na + Ka - 2CH_3]^+$, 2099.3 $[M_2 + 3Na + Ka - 2CH_3 - H]^+$, 2106.2 $[M_2 + 2Na + Ka - 2H]^+$, 2121.4 $[M_2 + 4Na + Ka - 2CH_3 - 2H]^+$, 2128.2 $[M_2 + 3Na + Ka - 3H]^+$, 2137.2 $[M_2 + 3Na + 2Ka - 2CH_3 - 2H]^+$ and 2144.3 $[M_2 + 2Ka + 2Na - 3H]^+$. Four peaks attributed to the trimer M_3: *m/z* 3155.3 $[M_3 + 2Ka + 2Na - 3H]^+$, 3163.4 $[M_3 + 2Ka + 3Na - CH_3 - 3H]^+$, 3177.4 $[M_3 + 2Ka + 3Na - 4H]^+$ and 3193.8 $[M_3 + 3Ka + 2Na - 4H]^+$. The supramolecular characteristic can also be observed in the MALDI-TOF mass spectrum

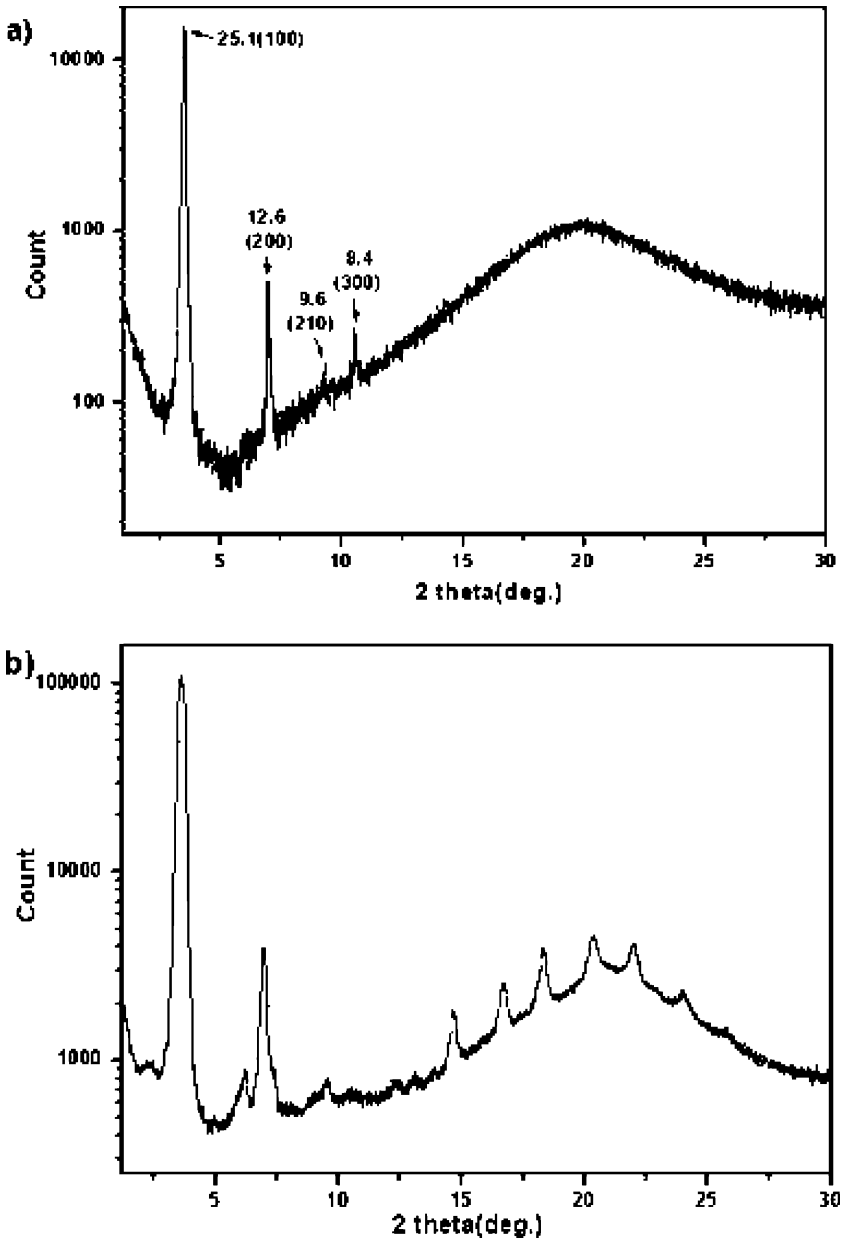

Figure 7. X-ray diffraction patterns of FH-T7 (a) at 150 and (b) at 25 °C on the first cooling run.

of FH-T3 (see the Supporting Information). Considering stacking interaction and tremendous steric repulsion between the trialkoxybenzoyl groups in neighboring molecules, rotation of the phenyl rings away from the bi-dihydrazine plane is necessary. In addition, the association constants in our case are somewhat small compared to that in other quadruple hydrogen-bonded systems, which might be attributed to the energy required for the out-of-plane rotation of the phenyl rings for stacking. Schematic representation of FH-Tn self-assembling to supramolecules was depicted in Scheme 3.

Mesomorphic Behaviors. The phase behaviors of FH-Tn ($n = 3, 6, 7, 8, 10$) were studied by differential scanning calorimetry (DSC) and polarizing optical microscopy and WAXD. The phase transition temperatures and the associated enthalpic changes for FH-Tn ($n = 3, 6, 7, 8, 10$) are summarized in Table 1. It can be seen that the phase behaviors were strongly affected by the length of the flexible terminal chains. FH-T3 is non-mesomorphic. On the other hand, FH-Tn ($n = 6, 7, 8, 10$) with longer alkoxyl terminal chains showed enantiotropic columnar phases. The clearing temperature decreased with the increase of the length of the alkyl chains. In addition, the DSC curves of FH-Tn ($n = 7, 8, 10$) exhibited obvious glass transition on the heating run, suggesting their supramolecular polymer characteristic (Figure 5), although the glass transition was not observed clearly during cooling. Figure 6a shows the optical textures of FH-T7 in its mesophase. The typically pseudo focal-conic texture with linear birefringent defects on slowly cooling from the isotropic liquid and the black areas, which are homeotropic domains with the columns aligned perpendicular to the glass substrates, suggest the characteristic of Col_h phases. Upon further cooling from the Col_h phase, a new phase developed without obvious morphology changes but with significant color changes. (Figure 6b).

The XRD pattern of FH-T7 at 150 °C showed one strong peak (25.1 Å) and three sharp weak peaks (12.6, 9.6, 8.4 Å) at larger angles (Figure 7a), which corresponded to a hexagonal columnar arrangement (Col_h) and a diffuse broad

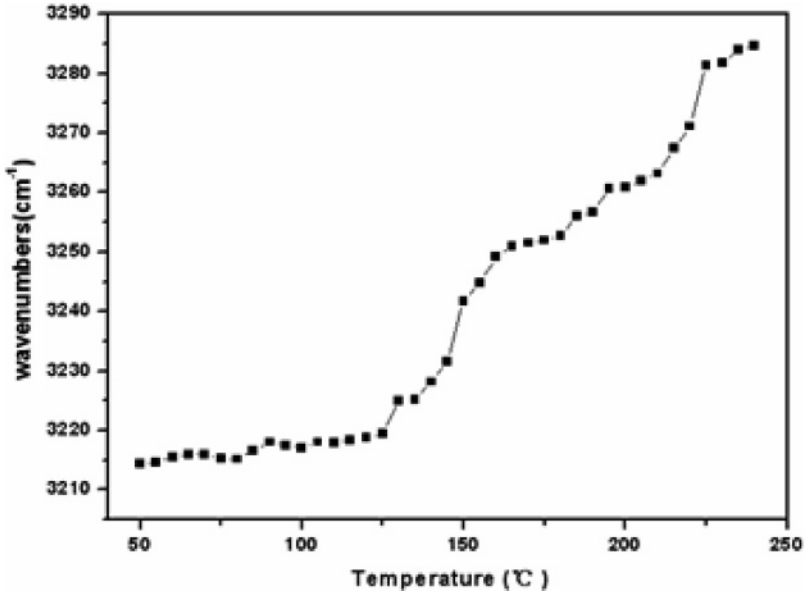

Figure 8. Temperature-dependent wavenumbers of N−H stretching vibrations of FH-T7.

Table 2. Powder WAXD Results of FH-Tn in Their Col_h Phases

compd	Col_h unit parameter *a* (Å)	d_{obsd} (Å)	d_{calcd} (Å)	Miller index
FH-T6 at 150 °C	27.5	23.8	23.8	100
		13.8	13.8	110
		11.9	11.9	200
		9.0	9.0	210
		7.9	7.9	300
		4.4 (halo)		
FH-T7 at 150 °C	29.0	25.1	25.1	100
			14.5	110
		12.6	12.6	200
		9.6	9.7	210
		8.4	8.4	300
		4.4 (halo)		
FH-T8 at 130 °C	30.2	26.2	26.2	100
			15.1	110
		13.1	13.1	200
		9.9	10.1	210
		8.7	8.7	300
		6.5	6.5	400
		4.5 (halo)		
FH-T10 at 140 °C	32.4	28.1	28.1	100
			16.2	110
		14.1	14.1	200
			10.6	210
		9.3	9.4	300
		4.5 (halo)		

peak with a maximum at about 4.4 Å was also observed, which is characteristic of the liquidlike arrangement of the aliphatic chains. At room temperature, some additional diffraction peaks at both low-angle and wide-angle regions were observed in the XRD patterns of FH-T7 (Figure 7b). However, we have no additional experimental evidence to assign the phases. Considering that an obvious glass transition was observed in DSC curves of FH-Tn (n = 7, 8, 10) on the heating run, we denote these phases as Col_x at lower temperature and glass (G) phase at room temperature. Similar phase structures were also observed for FH-Tn (n = 6, 7, 8, 10), and the XRD results of FH-Tn (n = 6, 7, 8, 10) in the Col_h phases are listed in Table 2. To investigate the intermolecular hydrogen bonds, we performed temperature-dependent FT-IR spectroscopy on FH-T7. Table 3 presented the assignments of infrared frequencies for FH-T7 on the second heating run at 50 °C. The presence of N−H stretching vibrations at 3214 cm^{-1} (the absence of free N−H, a relatively sharp peak with the frequency higher than 3400 cm^{-1}), intense absorption of amide I at 1626 cm^{-1}, and relatively weak absorption at 1693 cm^{-1} at 50 °C indicated that almost all the N−H groups are associated with C═O groups via N−H O═C hydrogen bonding.[22] The $\nu_s(CH_2)$ and $\nu_{as}(CH_2)$ appeared at 2857 and 2928 cm^{-1}, indicating disordered alkyl chains in the mesophases.[23] The wavenumbers of N−H stretching vibrations and amide I increased slightly in the glass and Col_x phases, whereas the increase is significant in the Col_h and isotropic phase with the increase in temperature (Figure 8.), indicating an increase in the average N−H O═C distance and intermolecular hydrogen bonds still remained in the Col_h phase as well as in the isotropic state near the clearing point.

Table 3. Assignments of Infrared Frequencies for FH-T7 at 50 °C

assignments	IR frequencies (cm^{-1})
ν(N−H)	3214
ν(Ar−H)	3016
$\nu_{as}(CH_3)$, $\nu_{as}(CH_2)$	2956, 2928
$\nu_s(CH_3)$, $\nu_s(CH_2)$	2871, 2857
amide I, νC═O	1693, 1629
νC═C of phenyl ring	1580
$\delta(CH_2)$	1468
	1428
CH_3 umbrella	1384
	1336
amide III, $\nu_{C-N}+\delta_{N-H}$	1234
ν(Ar−O)	1212
ν(C−O)	1114
	1004
$\delta(Ar-H)_{o.o.p,}$ *para-*	857
$\delta(Ar-H)_{o.o.p,}$ *mono-*	750
$(CH_2)_n$ rocking modes, $n \geq 4$	720

(22) (a) Skrovanek, D. J.; Howe, S. E.; Painter, P. C.; Coleman, M. M. *Macromolecules* **1985**, *18*, 1676−1683. (b) Harris, P. I.; Chapman, D. *Biopolymers (Pept. Sci.)* **1995**, *37*, 251−263.

(23) (a) Snyder, R. G.; Strauss, H. L.; Elliger, C. A. *J. Phys. Chem.* **1982**, *86*, 5145−5150. (b) MacPhail, R. A.; Strauss, H. L.; Snyder, R. G.; Elliger, C. A. *J. Phys. Chem.* **1984**, *88*, 334−341. (c) Venkataraman, N. V.; Vasudevan, S. *J. Phys. Chem. B* **2001**, *105*, 1805−1812.

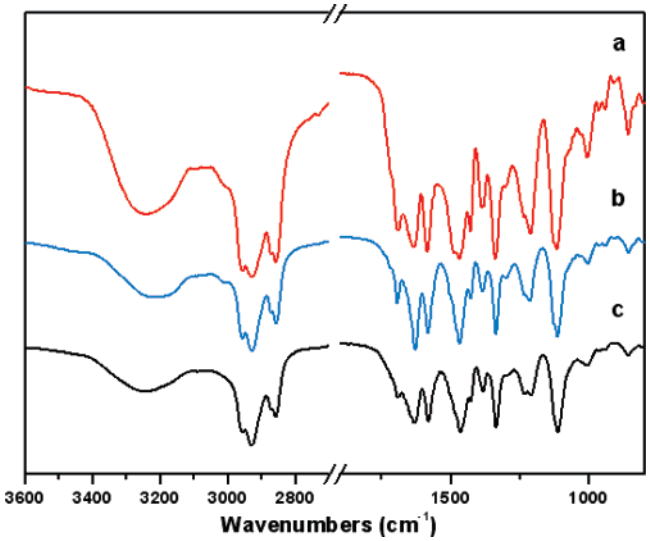

Figure 9. FT-IR spectra of FH-T7: (a) cast from chloroform at 25 °C, (b) glass phase at 55 °C, and (c) Col_h at 155 °C.

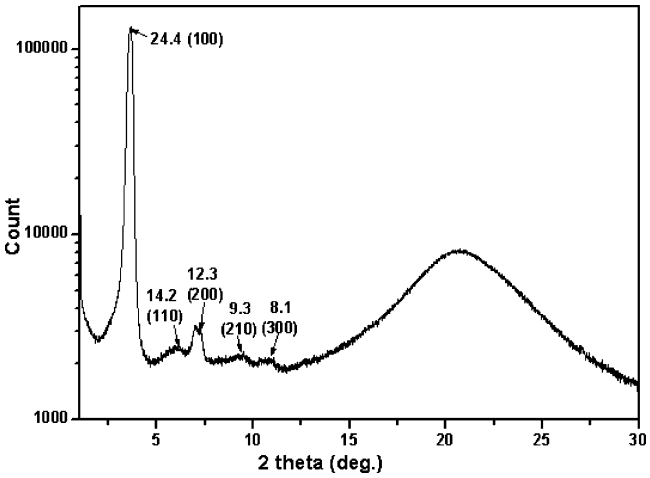

Figure 10. X-ray diffraction pattern of FH-T7 film casted from chloroform at 25 °C.

It is exciting to observe the column phase by air-drying the chloroform solutions of FH-T6 and FH-T7 at room temperature. The FTIR spectra of FH-T7 cast film from chloroform (Figure 9 a) was almost identical to that in Col_h phase; thus, molecules in the mesophases self-assemble into supramolecules in a way similar to that in chloroform. Interestingly, a hexagonal columnar arrangement (Figure 10) was observed in the cast film, although the *d* values are slightly smaller than that in its mesophase, which revealed that not only the self-assembled supramolecular structure but also the packing modes of the aggregates in both cases are the same. On the basis of the ^{1}H NMR diluting experiment, FTIR spectroscopy, and mass spectroscopy, we proposed that molecules self-assembling into supramolecular chains through intermolecular quadruple hydrogen bonding and the supramolecular chains arranged themselves into columnar mesophases.

Conclusion

The synthesis of a new twin-tapered compounds (FH-Tn) in which 3,4,5-trialkoxyl phenyl groups are linked to central bi-dihydrazide unit is described. It has been demonstrated that molecules were involved in intramolecular hydrogen bonding between amide groups in monomer, and there existed conformational transitions, e.g., from six-membered rings to five-membered rings intramolecularly H-bonding upon concentrating at lower concentrations (<255 μM). Results from ^{1}H NMR diluting experiments, FTIR spectroscopy, and mass spectroscopy revealed that intermolecular H-bonds are the main driving force for the formation of supramolecular chains of FH-Tn either in chloroform at higher concentrations or in bulk. Enantiotropic columnar phases were observed in FH-Tn (n = 6, 7, 8, 10) and room-temperature column hexagonal phases were obtained by air-drying the chloroform solutions of FH-T6, and FH-T7. These results suggested that bi-dihydrazide units could be used as self-complementary quadruple hydrogen-bonding units to assemble new supramolecules.

Acknowledgment. The authors are grateful to the National Science Foundation Committee of China (Project 50373016), Program for New Century Excellent Talents in Universities of China Ministry of Education, Special Foundation for PhD Program in Universities of China Ministry of Education (Project 20050183057), and Project 985-Automotive Engineering of Jilin University for their financial support of this work.

Supporting Information Available: DSC charts and X-ray diffraction patterns of FH-Tn (n = 3, 6, 7, 8, 10). ^{1}H NMR spectrum (500 MHz, 25°C) of FH-T7 in $CDCl_3$ at 120 μM. NOESY spectrum of FH-T7 (6.9 mM) in $CDCl_3$. MALDI-TOF mass spectrum of FH-T3 (Word document). This material is available free of charge via the Internet at http://pubs.acs.org.

CM062581I